Transactions on Computer Science and Intelligent Systems Research
ISSN: 2960-1800, eISSN: 2960-2238 | Volume 5
AIDML 2024

Optimization of submarine submersible search and rescue path based on simulated annealing

Yujun Yue *, Xingqi Dong

College of Computer & Information Science Southwest University, Southwest University, Chongqing, China, 400715

* Corresponding author: ygav063@gmail.com

Abstract. The aim of this paper is to apply models and algorithms to address the problem of searching and rescuing lost underwater vehicles. This paper main work is divided into three steps: establishing a geographic model, establishing a simulation model, and optimizing the search model. A model is built to predict the drift path of underwater vehicles in the ocean, and an optimization search model based on simulated annealing algorithm is used to find the optimal search and rescue strategy to locate the underwater vehicle in the shortest time possible. Experimental results demonstrate that by utilizing simulated annealing iterations and spatial physics analysis methods, it is possible to predict the path of underwater vehicles and identify the optimal search points, thereby improving rescue efficiency and rapidly locating the lost underwater vehicle.

Keywords: Discretizing; SA; Differential Equation; Probabilistic Circular Search.

1. Introduction

1.1. Background

Deep-sea exploration is full of risks and challenges, in the event of an accident on a submersible on a deep-sea expedition, the complexity of the ocean conditions makes the search and rescue mission extremely difficult. In 2023,a submersible named Titan suffered a catastrophic implosion on its way to the site of the Titanic, resulting in the deaths of five passengers, and a multinational search and rescue effort was unable to locate the wreckage of the victims. The incident has attracted widespread international attention. So we develop a safety procedures to deal with all contingencies encountered during deep-sea expeditions, including loss of contact and possible mechanical failures, in order to obtain regulatory approval. The safety procedures need to include accurate positioning of the submersible as well as rapid searching. Accurate positioning of the submersible after loss of contact and effective search and rescue teams will minimize casualties and property damage.

1.2. Related Work

Qinghua Luo et.al create a novel USBL positioning system with Kalman filtering for improved accuracy, utilizing a unique element array design and Kalman filters to enhance underwater target localization [1]. Mingzhen Xin et.al introduced a novel constant gradient sound ray tracing algorithm for underwater positioning, integrating a transcendental equation solution method to iteratively determine incident beam angles to achieve precise positioning [2]. Hongbo Yang et.al proposes a novel visual-based underwater positioning system utilizing a LiDAR camera and an inertial measurement unit, which, through sensor fusion and Bundle Adjustment method, accurately predicts submersible trajectories [3]. Tie Li et.al present a refined underwater positioning approach integrating sound wave transmission and reception disparities during circle-sailing, resulting in doubled observations and significantly enhanced precision [4]. Chengming Luo et.al investigate GLCCA for underwater positioning, aiming to optimize performance by integrating multiple methods such as inertial navigation, hydroacoustic positioning, and geophysical navigation [5].

1.3. Our Work

Our work focuses on addressing the problem of searching for and rescuing lost underwater vehicles by applying models and algorithms. The research is divided into three steps: establishing a geographic model, establishing a simulation model, and optimizing the search model. Firstly, we build a geographic model using ArcGIS software, with the Ionian Sea as the simulated target sea area. We import various data, including marine environmental data, seabed topographic data, and ocean current data, into ArcGIS for management and analysis. By processing and analyzing the geographic data, we deduce the direction and velocity of the ocean currents at different moments, which serves as one of the input parameters for predicting the path of the submersible. Secondly, we establish a simulation model for predicting the path of the submersible. We import the seafloor geo-environmental model from ArcGIS into MATLAB and divide the feasible sea area where the lost submersible could reach into a three-dimensional XYZ coordinate system. The force analysis of the submersible, considering gravity, buoyancy, ocean currents, and water resistance, is conducted in the x-axis direction. The resulting differential equation describes the motion of the submersible. By solving this equation, we obtain the displacement and velocity of the submersible at each iteration. Finally, we develop an optimal search model to minimize the search time for rescuing the lost submersible. When the submersible loses contact, we consider the host ship's position, denoted as R, and the initial deployment point for rescue boats and search equipment, denoted as D. Our goal is to find the coordinate position of D that minimizes the search time. Based on the path prediction and positioning model, we calculate the distance between D and the submersible's position at each iteration. By assuming a straight-line trajectory between the host ship and the rescue boat, we determine the distance between R and D. By utilizing simulated annealing iterations and spatial physics analysis methods, we can predict the path of underwater vehicles and identify the optimal search points. This approach significantly improves rescue efficiency and enables the rapid location of the lost underwater vehicle. Through the utilization of these models and algorithms, we successfully address the problem of searching for and rescuing lost underwater vehicles, improving rescue efficiency and minimizing casualties and property damage.

2. Preliminary

2.1. Assumptions

The lost submersible, influenced only by gravity, buoyancy, ocean currents, and water resistance during its drifting, stabilizes near obstacles upon contact. Its shape remains regular, ensuring consistent cross-sectional area (A) for water resistance. Upon reaching neutral buoyancy, the submersible steadies as velocity approaches zero. Both host ship and rescue boat maximize speed in straight courses for search and rescue operations.

2.2. Notations

The symbols used in this paper are shown in Table 1.

Table 1. Notations

Symbol	Description	Unit
W	The gravity of a submersible and its payload	N
F_B	The buoyancy of the submersible	N
F_{oc}	The force of the ocean current on the submersible	N
F_{water}	The resistance of the water to the submersible	N
v	The speed of the submersible	m/s
u	The speed of the ocean current	m/s
A	The cross-sectional area of the submersible	m^2
τ_{xx}	The component of the stress tensor	N/m^2
C_d	The coefficient of drag	
P_i, T_i	The location and time of the submersible after i iteration	
X^*, V^*	Initial position and velocity of the submersible	
X_i, V_i	The displacement and velocity obtained at the i iteration	
R	The initial position of the host ship on the surface of the sea	
D	The initial point to deploy the device and search	

3. Model building

3.1. Geographic Model

In this experiment, we will use the Ionian Sea as the simulated target sea area[6] .We use ArcGIS software as the main body to build a simulation geographic model of the Ionian sea and import the data into the solution software for subsequent solving of the model. The collected geographic data such as marine environmental data, seabed topographic data, and ocean current data will be imported into ArcGIS for management and analysis. The pertinent data for seawater density, ocean current velocity, and seafloor topographic elevation are meticulously acquired from esteemed oceanographic research institutions NOAA and NASA, satellite observations meticulously calibrated for current velocity assessments, and comprehensive bathymetric surveys supplemented by renowned databases such as GEBCO, ensuring the reliability and robustness of the input parameters for the submersible path prediction model integrated into the MATLAB solution software. Using the spatial analysis function of ArcGIS, the geographic data are processed and analyzed to deduce and encapsulate the direction and velocity of the ocean currents at different moments, and the obtained state of the ocean current motion is used as one of the input parameters to establish the prediction model for the path of the submersible.

3.2. The establishment of simulation model

In order to build a predictive model for the path of the submersible, we imported various data from the seafloor geo-environmental model built from ArcGIS into MATLAB to be solved, and divided the part of the sea area where the lost submersible could reach to build a three-dimensional XYZ coordinate system, with the Z-axis encompassing the entire distance from the deepest point of the seafloor to the sea level. We divided the feasible domain D_n according to the area encompassed by seawater, implying that the predicted paths can only be generated where seawater is present.

First of all, the force analysis of the submersible, due to the loss of the propulsion of the submersible, so at this time the submersible is only subject to gravity W, buoyancy F_B, the force of the ocean current $F_{oc}$and the resistance of the water F_{water}. In the xyz three-dimensional coordinate system, we only need to analyze the x-axis direction of the force and the movement of the situation can be, yz direction can be derived by analogy. In the direction along the x-axis, the forces on the various forces are represented as follows [7].

$$
\begin{cases}
W_x = mg_x \\
F_{B_x} = \rho_{sea} g_x V \\
F_{oc_x} = \frac{\partial \rho_{sea} u_x}{\partial t} + \frac{\partial \rho_{sea} u_x^2}{\partial x} + \frac{\partial p}{\partial x} - \frac{\partial \tau_{xx}}{\partial x} - \rho_{sea} g_x \\
F_{water_x} = \frac{1}{2} C_d \rho_{sea} A (v_x - u_x)^2
\end{cases} \tag{1}
$$

From the vector expression of the system of equations (1), the combined force along the x-axis is given as:

$$
F_{total_x} = \overrightarrow{W_x} + \overrightarrow{F_{B_x}} + \overrightarrow{F_{oc_x}} + \overrightarrow{F_{water_x}} \tag{2}
$$

The force analysis of the submersible's un-powered motion process is shown in Fig. 1.

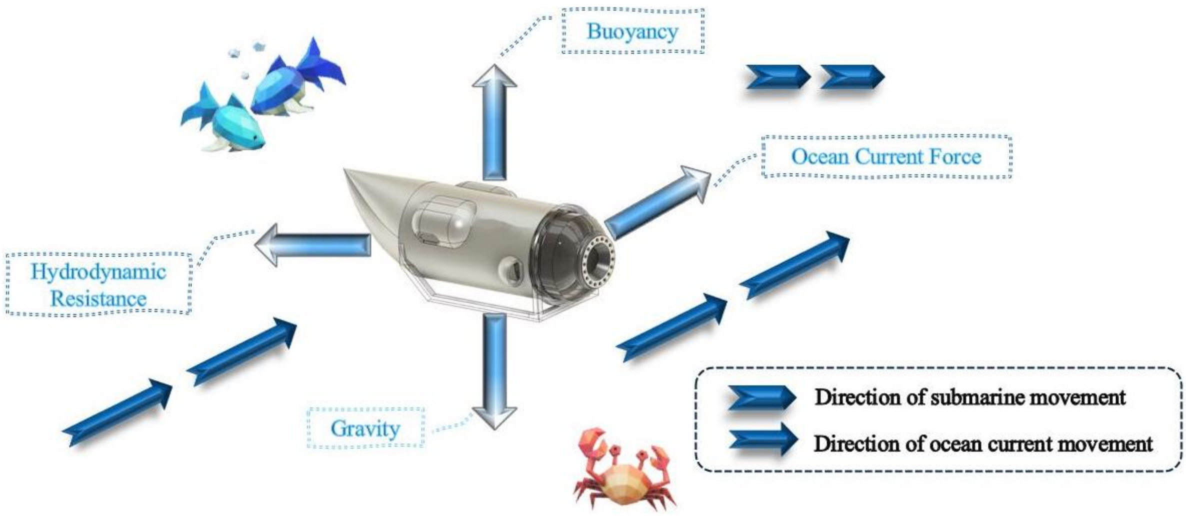

Figure 1. Force analysis diagram

From Newton's laws of motion, we have $F_{total_x} = ma_x$, and because of $a_x = \frac{\partial v_x}{\partial t}$, a differential equation can be built from this:

$$
F_{total_x} = m \frac{\partial v_x}{\partial t} \tag{3}
$$

3.3. Optimal Search Model

When the host ship finds that the submersible has lost contact, we consider the point at which the host ship randomly appears in the sea level patrol area, defined as $R = (x_r, y_r, H)$, H is the ocean depth at that location, and the position of the host ship is fixed at point R. Then we set the initial point on the sea to deploy rescue boats and other search equipment is $D = (x_d, y_d, H)$, and our goal is to get a coordinate position D to minimize the search time.

In order to minimize the search and rescue time, we believe that the host ship and the rescue boat sent are in a straight line, and it is easy to know that the distance from the host ship position R to the deployment point D is $\|R - D\|_2$. According to the path prediction and positioning model established in our first question, it can be obtained that the position of the submersible is P_i at time $T_i = i\Delta t$, and then the distance between the deployment point D and the submersible is $\|P_i - D\|_2$.

The speed of the host ship with deep-sea exploration function is usually able to reach 10 to 15 knots, equivalent to 5 to 8 meters per second, and the speed of the underwater search equipment is usually between 1 and 4 knots, equivalent to about 0.5 to 2 meters per second. Due to the urgency of the rescue operation, we set the speed of the host ship to $V_h = 8m/s$ and the speed of the rescue boat to $V_r = 2m/s$.

Based on the above data, it can be calculated that the total time $T^*(i)$ for the host ship to receive the rescue signal (i.e. the submersible loses contact), then release the rescue boat through the deployment point, and finally the rescue boat reaches the anchor point of the submersible is:

$$T^*(i) = \frac{\|R-D\|_2}{V_h} + \frac{\|P_i-D\|_2}{V_r} \tag{4}$$

The simulated annealing algorithm will search the optimal solution of the deployment point in the search and rescue route established by us according to the objective function and constraints, so that the rescue boat can reach the predicted location of the submersible in the shortest time. We need to define the objective function and constraints in the simulated annealing algorithm to obtain the optimal solution of the deployment point. We define the objective function and constraints as follows:

$$Objective\ function \qquad Minimize\ T^*(i) \tag{5}$$

$$Subject\ to. \qquad T^*(i) = T_i, i = 1,2 \ldots n \tag{6}$$

The algorithm generates an adjacent solution, update $D = (x_d, y_d, H) \to D = (x_d + \Delta x, y_d + \Delta y, H), \Delta x, \Delta y \to 0$, by making a small disturbance near the initial deployment point D. The simulated annealing temperature indicates the degree of exploration of the search. Set the initial temperature to 100°C and the temperature drop policy to adaptive drop [8].

The simulated annealing algorithm is used for iterative search. In each iteration, adjacent solutions are generated based on the neighborhood operations of the current solution.

Repeat this process until the maximum number of iterations is reached.

From this, we get the optimal sea surface deployment point $D^* = (x_d^*, y_d^*, H)$, and the shortest time $T^*(i) = i\Delta t$ can be calculated by the return value i.

4. Process

The basic idea of the numerical method is to discretize the time-continuous problem and approximate the continuous solution by iterative computation. Within each relatively small time step Δt, the position and velocity of the submersible are updated using numerical approximations of the differential equations. In this way, the trajectory of the submersible in time is obtained.

Based on the idea of discretization and the idea of solving by numerical methods, equation (1) is organized into equation (7):

$$\int_0^{\Delta t} F_{total_x} \partial t = \int_{v_x}^{v_{x_1}} m \partial v_x \tag{7}$$

Where Δt is the time step of each iteration; v_x is the velocity along the x-axis when the submersible was lost, which is used as the initial velocity for the iterative computation; and v_{x_1} is the velocity of the submersible along the x-axis after Δt of the first iteration.

The displacement for the first iteration can be obtained from the v_{x_1} calculated for the first iteration as:

$$x_1 = \frac{(v_x + v_{x_1})}{2} \Delta t \tag{8}$$

By analogy, the second iteration takes v_{x_1} as the initial velocity of (7) for the same step size Δt, and the displacement of the second iteration can be obtained x_2. The termination condition of the iteration in the x-axis direction is that $v_{x_{n+1}}$ tends to zero.

Extend the differential equation to the three-dimensional XYZ coordinate axis, in the ith iteration to get x_i at the same time to get y_i and z_i, which means that in the ith iteration, the submersible moves in the direction of (x_i, y_i, z_i), the distance moved to $\sqrt{x_i^2 + y_i^2 + z_i^2}$. When the three directions of the initial velocity of the next iteration tends to 0, the overall iteration is over, and the submersible may reach the neutral buoyancy point in the ocean at this time. At this point, the direction and distance of each iteration can be superimposed to obtain a relatively smooth trajectory, this trajectory is our prediction of the submersible's movement path, the total movement time $T = n\Delta t$, where n is the number of iterations. During the i iteration, we can also get the position and time of the submersible under this iteration in real time as follows:

$$\begin{cases} P_i = X^* + X_1 + X_2 + \ldots + X_i \\ T_i = i\Delta t, i \epsilon N \end{cases} \tag{9}$$

Where P_i is the location of the submersible after the ith iteration,T_i is the time elapsed in the i-th iteration, $X^* = (x^*, y^*, z^*)$ is the initial location of the submersible lost, and $X_1 = (x_1, y_1, z_1) \sim X_i = (x_i, y_i, z_i)$ is the result obtained in each iteration.

where $V^* = (v_x^*, v_y^*, v_z^*)$ is the initial velocity vector of the submersible at the time of loss, of size $\sqrt{v_x^{*2} + v_y^{*2} + v_z^{*2}}$.

We randomly give the initial position of the lost submersible (0.483, -1.875, 9.201), the dive velocity v=1.556m/s to simulate the simulation experiment, and compare it with the ArcGIS current simulation run result map, in which the blue trajectory is the result of our algorithm execution, and the red trajectory is the result of the ArcGIS simulation run, see Fig.2.

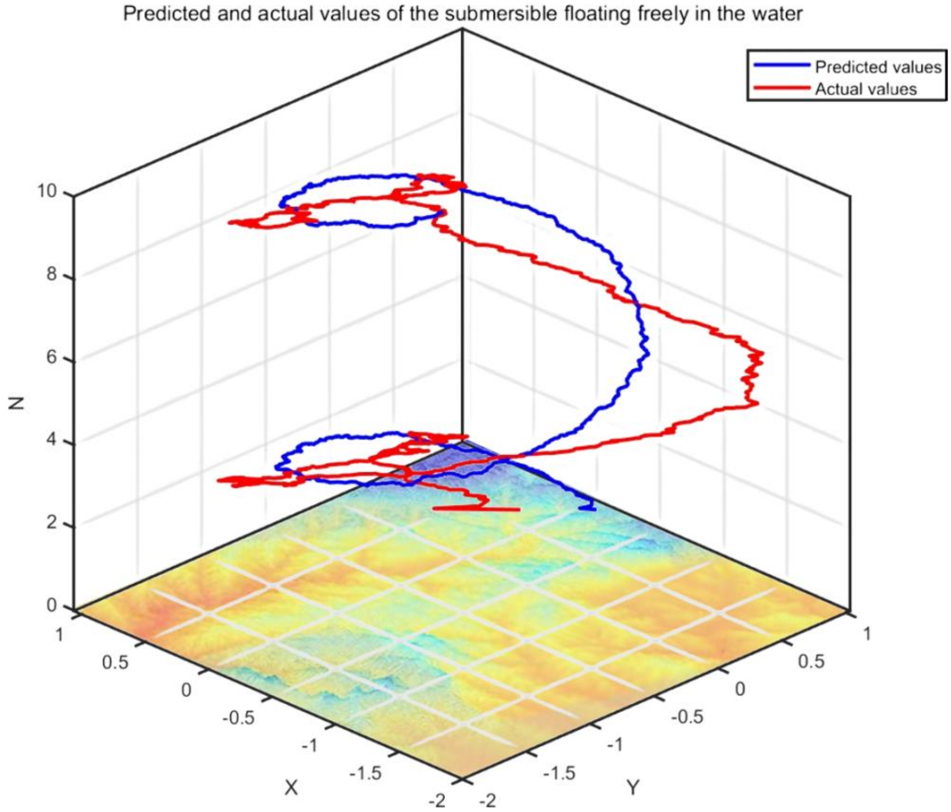

Figure 2. Path prediction figure

Through the previous model, we found an optimal launch point for rescue boats. The rescue boat then travels in a straight line to the submersible prediction point at time $T^*(i)$.

After the search equipment reached the predicted point of the submersible, we designed and optimized the path of the seabed search from that point to reduce the search time and resource consumption.

For the selection of underwater search route, we first simulate the free floating path of the submersible in the sea, and then calculate the probability of the submersible appearing at other positions on the same level at each point on the outlet line according to the previous uncertainty. With the point on the path as the radius, the probability of the submersible's presence decreases with the increase of the search radius. We set the threshold for terminating the search with a probability of 70%, when the search radius $R > R_{70\%}$ terminates the search for that plane. The disk search of this pattern continues from the prediction point $T^*(i+1)$. The probability distribution diagram of underwater search mode on the same plane is shown in Fig.3:

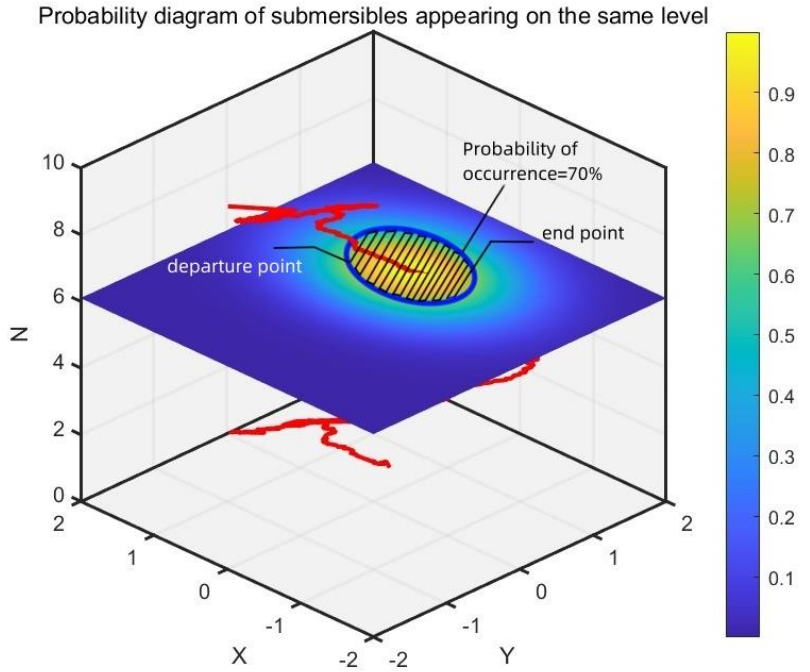

Figure 3. Search pattern probability graph

In the figure, the red curve is the predicted path of the lost submersible, the black square curve is the search route of the search equipment, and the interval D between each black parallel line is the maximum scanning distance of the search and rescue equipment. The departure point is connected to the end point of the previous search layer, and the end point is connected to the departure point of the next search layer. The probability of a lost vehicle appearing in the dark blue oval is 70%.

By changing the seabed conditions and the location of the loss of contact, we simulated the search process under different conditions and obtained different search times. For each simulated search time, we counted the number of underwater vehicles found in the same time, and obtained the distribution of search times at each time point, the simulation results are available at Fig.4(a).

To understand in more detail the probability of a submersible being found in relation to time and cumulative search results, we calculated the sum of searches at each time point and all time points before it as a percentage of the total number of simulations and show the probability of finding a submersible in Fig.4(b).

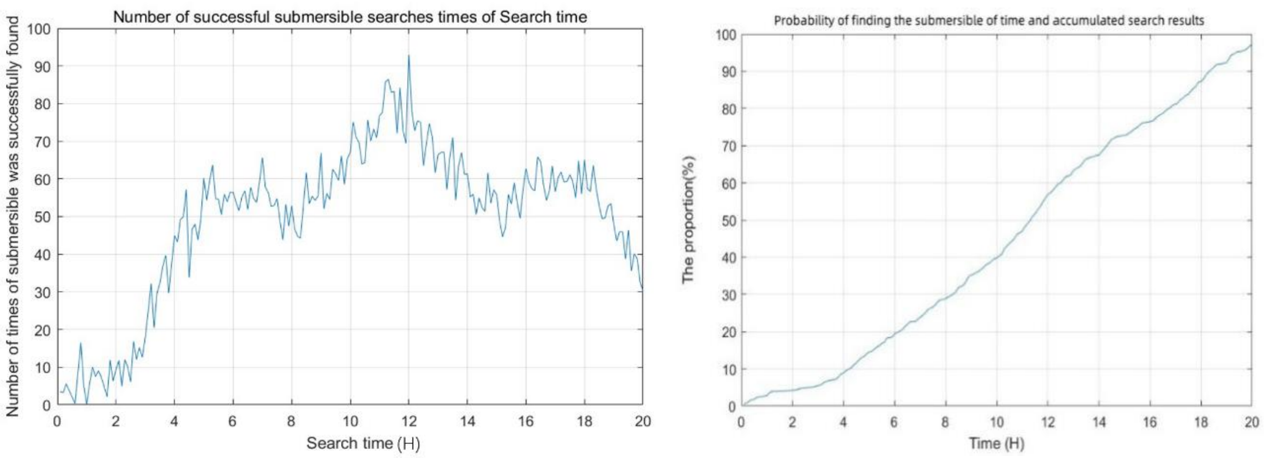

(a) Search results at every moment (b) Probability of finding a submersible

Figure 4. Determination of probability function

By fitting the curve of this ratio over time, a more detailed functional relationship between the probability of submersible being found and time is obtained as follows:

$$P(t) = 5.81t^2 + 420.58t - 597.3 \tag{10}$$

We evaluated the sensitivity of the model to changes in input parameters to determine the impact of each parameter on the model results. We performed sensitivity analysis for the following parameters. We change the initial position to assess its impact on the lost vehicle position prediction and search results. We adjust ocean velocity to see how it affects the path of the missing submersible and the search results. We analyzed the influence of C_d on the drift and path prediction of the lost submersible. We studied the effect of submersible speed on search effectiveness and search time. We consider the effect of shape of submersibles on water resistance and drift processes [9].

The local sensitivity index measures the sensitivity of the model output to a single parameter. For parameter θ, the local sensitivity index formula is:

$$S_\theta(x) = \frac{\partial f(x)}{\partial \theta} \cdot \frac{\theta}{f(x)} \tag{11}$$

Where $f(x)$ is the output of the model, x represents the input of the model, and the partial derivative $\frac{\partial f(x)}{\partial x}$ is calculated by finite difference.

After the local sensitivity index is obtained, if the absolute value of $S_\theta(x)$ is larger, it means that parameter θ has a greater influence on output $f(x)$. If the absolute value of $S_\theta(x)$ is small, it means that parameter θ has less influence on output $f(x)$.

The calculated local sensitivity indexes of each parameter are shown in the following table:

Table 2. local sensitivity index

initial position	ocean velocity	C_d	Submersible speed	Submersible shape
0.921	0.085	0.113	0.162	0.057

According to the local sensitivity index, and after comparison with Table 2, the Submersible Path Prediction Model and Optimal Search Model are sensitive to the change of the initial position of the submersible and can cope with the sudden loss of contact in time. The sensitivity of four parameters, ocean velocity, C_d, submersible speed and shape of submersible, is low, indicating that the model can be widely used in different sea areas and different types of submersibles [10].

5. Conclusion

In conclusion, this paper presents a safety procedure of submersible loss of contact or machine failure. The procedure includes a positioning model for predicting the submersible's position over time and an optimal search model for deployment and search location recommendations. This comprehensive approach enhances the safety of deep-sea expeditions and can be applied to other similar scenarios. The model only considers that the submarine is only affected by gravity, buoyancy, ocean current force and water resistance during the drifting process, and ignores other complex factors. And it doesn't take into account the complexity of what happens when submarine hit an obstacle.

References

[1] Luo Q, Yan X, Ju C, Chen Y, Luo Z. An Ultra-Short Baseline Underwater Positioning System with Kalman Filtering [J]. Sensors (Basel), 2020, 21 (1): 143.

[2] Mingzhen XIN, Fanlin Y, Shuqiang XUE, et al. A constant gradient sound ray tracing underwater positioning algorithm considering incident beam angle [J]. Acta Geodaetica et Cartographica Sinica, 2020, 49 (12): 1535.

[3] Yang H, Xu Z, Jia B. An Underwater Positioning System for UUVs Based on LiDAR Camera and Inertial Measurement Unit [J]. Sensors, 2022, 22 (14): 5418.

[4] Li T, Zhao J, Ma J. A precise underwater positioning method by considering the location difference of transmitting and receiving sound waves [J]. Ocean Engineering, 2022, 247: 110480.

[5] Luo C, Wang L, Yang X, et al. Underwater data-driven positioning estimation using local spatiotemporal nonlinear correlation [J]. IEEE/CAA Journal of Automatica Sinica, 2023, 10 (8): 1775 - 1777.

[6] Lycourghiotis S. Sea Topography of the Ionian and Adriatic Seas Using Repeated GNSS Measurements [J]. Water, 2021, 13 (6): 812.

[7] Chu Z, Wang F, Lei T, et al. Path planning based on deep reinforcement learning for autonomous underwater vehicles under ocean current disturbance [J]. IEEE Transactions on Intelligent Vehicles, 2022, 8 (1): 108 - 120.

[8] Guilmeau T, Chouzenoux E, Elvira V. Simulated annealing: A review and a new scheme [C]//2021 IEEE Statistical Signal Processing Workshop (SSP). IEEE, 2021: 101 - 105.

[9] Razavi S, Jakeman A, Saltelli A, et al. The future of sensitivity analysis: an essential discipline for systems modeling and policy support [J]. Environmental Modelling & Software, 2021, 137: 104954.

[10] Valkó É, Varga T, Tomlin A S, et al. Investigation of the effect of correlated uncertain rate parameters via the calculation of global and local sensitivity indices [J]. Journal of Mathematical Chemistry, 2018, 56 (3): 864 - 889.